analytical chemistry

Technical Note

Cite This: *Anal. Chem.* 2019, 91, 5537−5541

pubs.acs.org/ac

Diamond Colloidal Probe Force Spectroscopy

Peter Knittel,* Taro Yoshikawa, and Christoph E. Nebel

Fraunhofer IAF, Institute for Applied Solid State Physics, Tullastraße 72, 79108 Freiburg, Germany

Supporting Information

ABSTRACT: Diamond is a highly attractive coating material as it is characterized by a wide optical transparency window, a high thermal conductivity, and an extraordinary robustness due to its mechanical properties and its chemical inertness. In particular, the latter has aroused a great deal of interest for scanning probe microscopy applications in recent years. In this study, we present a novel method for the fabrication of atomic force microscopy (AFM) probes for force spectroscopy using robust diamond-coated spheres, i.e., colloidal particles. The so-called colloidal probe technique is commonly used to study interactions of single colloidal particles, e.g., on biological samples like living cells, or to measure mechanical properties like the Young's modulus. Under physiological measurement conditions, contamination of the particle often strongly limits the measurement time and often impedes reusability of the probe. Diamond as a chemically inert material allows treatment with harsh chemicals without degradation to refurbish the probe. Apart from that, the large surface area of spherical probes makes sensitive studies on surface interactions possible. This provides detailed insight into the interface of diamond with other materials and/or solvents. To fabricate such probes, silica microspheres were coated with a nanocrystalline diamond film and attached to tipless cantilevers. Measurements on soft polydimethylsiloxane (PDMS) show that the manufactured diamond spheres, even though possessing a rough surface, can be used to determine the Young's modulus from a Derjaguin-Muller-Toporov (DMT) fit. By means of force spectroscopy, they can readily probe force interactions of diamond with different substrate materials under varying conditions. The influence of the surface termination of the diamond was investigated concerning the interaction with flat diamond substrates in air. Additionally, measurements in solution, using varying salt concentrations, were carried out, which provide information on double-layer and van-der-Waals forces at the interface. The developed technique offers detailed insight into surface chemistry and physics of diamond with other materials concerning long and short-range force interactions and may provide a valuable probe for investigations under harsh conditions but also on biological samples, e.g., living cells, due to the robustness, chemical inertness, and biocompatibility of diamond.

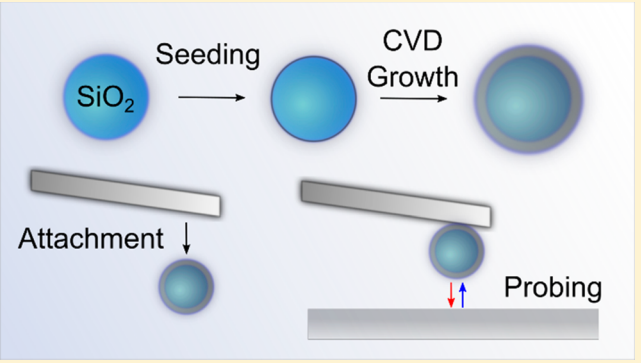

In the last 2 decades, the so-called colloidal probe technique has developed into an indispensable tool for biological and materials research.[1] For this technique, commonly, a single colloidal particle is attached to a tipless cantilever and used in force spectroscopic measurements employing an atomic force microscope (AFM).

Probing forces between single colloids and substrates provides insight into interfacial properties like substrate adhesion, electrostatics, and hydration but also mechanical properties of soft matter, e.g., living cells or polymer films.[2,3] Using soft AFM cantilevers, due to the large contact area, interfacial forces down to the piconewton range can be investigated in detail. This has been used for sensitive studies on fouling resistant membranes and coatings,[4] wettability properties,[5] bubbles in liquid,[6] and conductive polymer coatings,[7] to name a few. However, measurements are often strongly affected by the lifetime of the colloidal probe, which limits the measurement time and requires frequent preparation of fresh probes. Especially when measuring on living cells, only a few reliable data points can be obtained[8] and hence methods for rapid colloid exchange have been developed.[9]

In this study, we introduce diamond colloidal probe force spectroscopy, using a robust and chemically inert diamond sphere attached to a tipless AFM cantilever for probing. Diamond is a common coating material for AFM probes as it is exceptionally hard (Young's modulus, 1220 GPa) and wear resistant.[10] Apart from that, heavily doped diamond shows metal-like conductance and outstanding electrochemical properties. Therefore, it has been used to fabricate conductive tips or serves as electrode material in combined techniques like AFM-scanning electrochemical microscopy (AFM-SECM).[11]

Even though it is termed as chemically inert, chemical modifications are feasible, e.g., for chemical force spectroscopy.[12] It was also shown that proteins in fetal bovine serum can easily adsorb onto the diamond surface.[13] Thermal or plasma

Received: February 6, 2019
Accepted: April 10, 2019
Published: April 10, 2019

DOI: 10.1021/acs.analchem.9b00693
Anal. Chem. 2019, 91, 5537−5541

treatments can readily modify the surface, e.g., for hydrogen or oxygen termination.[14,15] Especially, hydrogen-terminated diamond has some outstanding properties. It is characterized by strong hydrophobicity, shows surface conductivity,[16] and a negative electron affinity (NEA) that can be used for chemical reactions, e.g., CO_2 reduction, by emission of electrons into solution.[17] Depending on the surface termination, also the interaction with other materials, solvents, and molecules can be significantly altered. This is even more important for nanomaterials, where surface states dominate the overall behavior. With diamond colloidal particles, detailed characterization of surface properties like terminations and dynamics, e.g., degradation of hydrogenated diamond,[18] is feasible but also a robust probe for investigations under harsh conditions is readily available.

EXPERIMENTAL SECTION

Sample Preparation. For the manufacturing of micrometer-sized diamond spheres, a templated growth method was used that was adapted from our previous studies.[19,20] The 5 μm silica beads in suspension (50 mg/mL, Kisker Biotech GmbH & Co KG, Germany) were centrifuged at 4000 rpm for 5 min to separate them from the solution. Then, they were cleaned in a 5:1:1 mixture of water, ammonia, and hydrogen peroxide to remove organic contaminants and to oxidize the surface. After separation from the cleaning solution by centrifugation, the silica spheres were seeded using an aqueous nanodiamond solution (4 nm nanodiamonds, G01 grade, Plasmachem GmbH, Germany) and gentle ultrasonic treatment.[21] The seeded spheres were again centrifuged and rinsed with ultrapure water two times before being suspended in 10 mL of isopropanol (5 mg/mL). A volume of 1 mL of this suspension was spin-coated (3000 rpm, 30s) onto a 3 in. double-side polished silicon wafer and dried in air.

Growth of Diamond Spheres, Pretreatment, and Mounting. Diamond growth was carried out for 30 min in an ellipsoidal microwave plasma chemical vapor deposition (MPCVD) reactor using purified gases (H_2, CH_4) with 3.4 kW microwave power, 3.5% CH_4 in H_2 and a chamber pressure of 65 mbar.[22] The overgrown particles were then removed from the silicon substrate by an ultrasonic treatment and suspended in isopropanol. For further treatments and attachment, the suspension was drop-coated onto a piece of silicon wafer. O-termination was achieved in an O_2-asher (100-E, TePla, Germany) at 200 W power with an O_2 pressure of 1 mbar for 10 min. H-termination was carried out in the MPCVD reactor in an H_2-plasma for 10 min at 1.3 kW and 40 mbar. Afterward the treated substrates were mounted in a JPK NanoWizard III AFM (JPK, Germany), and the spherical diamond particles were attached to tipless AFM cantilevers (HQ:CSC38/tipless/Cr−Au, k = 0.003−0.130 N/m, MikroMasch, Bulgaria) using a UV-curable glue (OP-4-20641, Dymax). All used diamond spheres were taken from the same batch and should have a similar roughness of 18 ± 2 nm (see also Figure 1 and Figure S1).

Force Spectroscopic Measurements. After attachment, each diamond particle was characterized by scanning electron microscopy (SEM). Then, the probe was calibrated using the thermal noise method.[23] The measurements on diamond were carried out on an approximately 1 × 1 cm^2 large piece of polished polycrystalline diamond (PCD) pretreated by H_2-plasma (using the same conditions as for the diamond spheres) or wet-chemical oxidation, using a mixture of 1:3 nitric acid and sulfuric acid at 250 °C. In air and solution, the force spectroscopy was conducted with a set point force of 5 nN and a tip velocity of 1 μm/s. The used probes (Figure S5) had a spring constant of 0.09 N/m and 0.14 N/m (for the oxygenated and hydrogenated diamond sphere, respectively). For the elasticity measurements, a commercially available, soft polydimethylsiloxane (PDMS) sample was used (2.5 MPa, Bruker S.A.S., France). Here, the hydrogenated probe was employed and a set point force of 50 nN and a tip velocity of 1 μm/s were chosen. Data processing and evaluation was carried out from 20 to 40 force curves with the JPK Data Processing software. For evaluating the force range in solution, an increase by 25 pN was determined, which is above the noise of approximately 15 pN and not influenced by spikes.

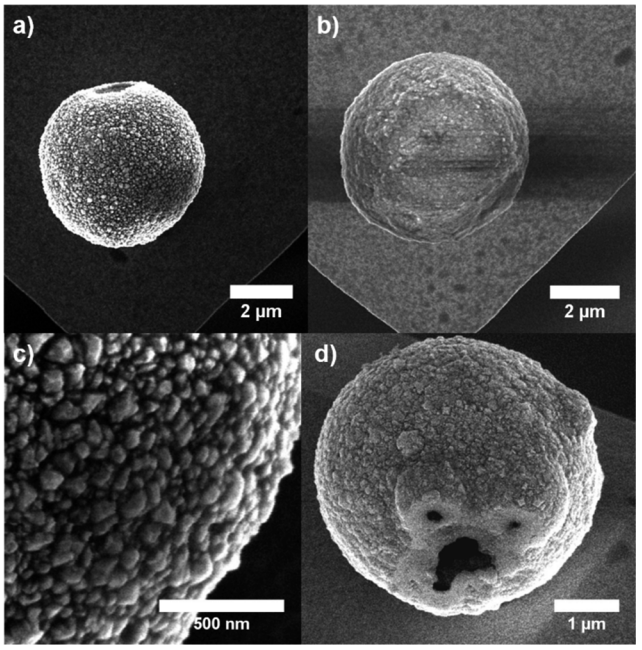

Figure 1. SEM images of diamond coated silica spheres attached to tipless AFM cantilevers: (a) H-terminated diamond layer and (b) O-terminated diamond layer. (c) Single crystallites in a zoomed view of the H-terminated diamond. (d) Hollow diamond sphere after removal of the silica core in 25% hydrofluoric acid (tilt angle, 45°).

RESULTS AND DISCUSSION

Templated diamond growth on silica is a well-established technique and has been used before to obtain, e.g., highly porous diamond substrates like foams or membranes[19,24] but also individual fibers.[25] This is readily achieved by controlling the surface coverage of the template with nanodiamonds (i.e., seeding).[20] Using 5 μm spherical silica particles seeded with nanodiamonds, diamond coated spheres were grown on a silicon wafer. The coating was then hydrogenated or oxygenated using a plasma treatment before attachment to a tipless AFM cantilever.

Characterization using SEM shows the successful positioning at the end of the cantilever (Figure 1a). Also, the surface termination shows a strong influence on the contrast of the SEM images. Whereas the H-terminated colloidal particle (H-colloid) shows strong contrast of the individual diamond crystallites, the O-terminated colloidal particle (O-colloid) exhibits charging effects and less contrast. This is due to the

DOI: 10.1021/acs.analchem.9b00693
Anal. Chem. 2019, 91, 5537−5541

surface conductivity of H-terminated diamond and proves the successful pretreatment of the spheres before attachment.[16]

The grown diamond layer has a crystalline structure with crystallite sizes in the range of 50−150 nm (Figure 1c). Due to the 3-dimensional template making contact with the wafer, the particle is truncated on one side where no diamond was grown (Figure 1a). Apart from that, the diamond layer on the sphere is homogeneous with 200−300 nm thickness and does not show degradation from the plasma treatments (Figure 1c and Figure S1). Due to the truncation, the silica core may be readily removed by etching with hydrofluoric acid (Figure 1d).

The colloidal probe technique is commonly used to investigate mechanical properties as the spherical shape ideally fits to the Hertz model of elastic deformation.[26] In air, strong adhesive capillary forces are present. The Derjaguin-Muller-Toporov (DMT) model considers adhesion and provides the Young's modulus according to eq 1:[27]

$$F - F_{adh} = \frac{4}{3}\frac{E}{1-\nu^2}\sqrt{R}\delta^{3/2} \quad (1)$$

F is the applied force, F_{adh} the adhesion force, ν the Poisson's ratio (0.5), E the Young's modulus, R the radius of the sphere (2.7 μm), and δ the indentation depth. Due to the large surface area, the colloidal probe also offers the advantage of exerting lower pressure, which becomes important when probing fragile samples.

To investigate the indentation behavior of the diamond colloid, a commercially available, soft PDMS sample was probed and a DMT fit was carried out from the obtained approach curves (Figure 2). The obtained Young's modulus of 2.59 ± 0.06 MPa is in excellent agreement with the value specified by the manufacturer (2.5 ± 0.7 MPa) (see also Table S2).

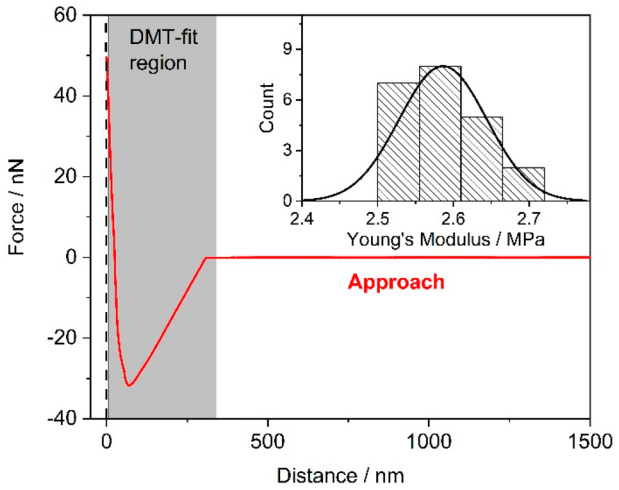

Figure 2. Measurement conducted on elastic PDMS (Young's modulus, 2.5 MPa ± 0.7 MPa) and representative approach curve. Inset shows the data obtained from 22 measurements after DMT fitting.

From the SEM images (Figure 1), the difference in surface termination is clearly visible. In the literature, it was shown that O-terminated diamond is hydrophilic and H-terminated diamond is hydrophobic.[28] Thus, the fabricated probes should show different adhesion behavior in air (where meniscus forces dominate). To further investigate the influence of the pretreatment, force spectroscopic measurements on H- and O-terminated PCD (HPCD, OPCD) were carried out. All obtained force−distance curves exhibit clear differences as shown in Figure 3. For an O-colloid, we observed the lowest

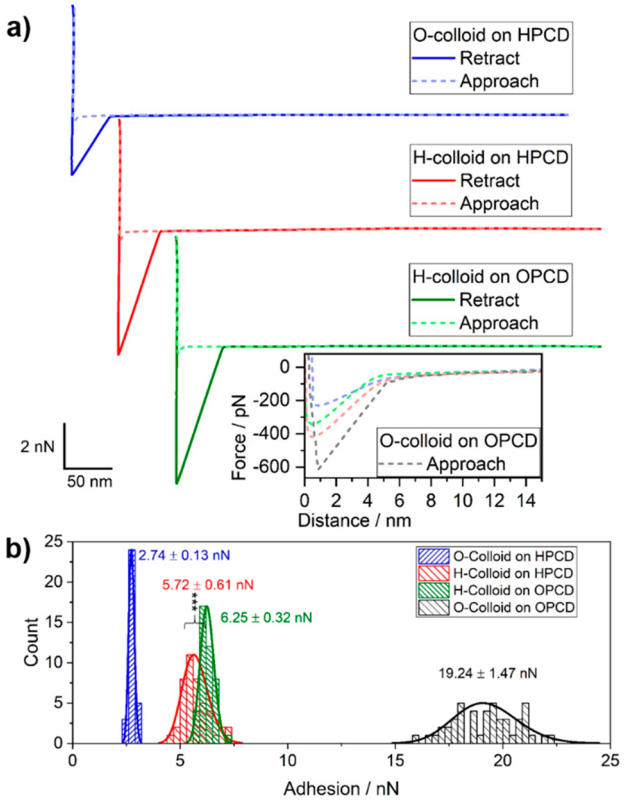

Figure 3. Force spectroscopic measurements using O- and H-terminated colloids and diamond samples in air. (a) Representative force curves for the different surface terminations showing approach and retract (inset shows magnified view of the approach traces). (b) Statistical data of the measured adhesion. Note: In part a, for the O-colloid and OPCD where the adhesion force is significantly higher, only the approach part is shown in the inset for better presentation.

adhesion with 2.74 ± 0.13 nN in all measurements on HPCD, whereas on an OPCD surface, the measured force was the largest with 19.25 ± 1.47 nN. For the H-colloid on the OPCD, 6.25 ± 0.32 nN was obtained. These trends can be explained by the wettability of the substrates, i.e., the different capillary forces. Equation 2 describes these forces (F) in a sphere-plane geometry:[29]

$$F = 4\pi R\gamma\cos(\theta) \quad (2)$$

R is the radius of an ideal sphere, γ the surface tension of water (71.99 mN/m),[30] and θ the meniscus contact angle. It was shown in other studies that, for rough colloids, the actual colloid radius needs to be replaced by the radius of the nanoscale asperities.[29] With R = 20 nm (see also Figure S1) and a meniscus contact angle of 0°, this results in a capillary force of 18.09 nN (O-colloid on OPCD). A contact angle of 81.3° and 69.8° yields a capillary force of 2.74 nN (O-colloid on HPCD) and 6.25 nN (H-Colloid on OPCD), respectively. The calculations are in good agreement with the obtained measurements and literature data.[31] For the H-colloid on OPCD, the slightly decreased contact angle may be caused by the difference between nanocrystalline diamond and PCD or

DOI: 10.1021/acs.analchem.9b00693
Anal. Chem. 2019, 91, 5537−5541

by a minor surface oxidation during probe preparation (UV treatment).

The H-colloid shows an adhesion force of 5.72 ± 0.61 nN on the HPCD (distribution is significantly different from H-colloid on OPCD on a significance level of $\alpha = 0.001$). Due to the hydrophobicity of both substrates, the meniscus forces should be comparably low. The rather high adhesion may be explained by the microscopic structure of water on hydrophobic surfaces, where nanodroplet formation has been observed.[32] These droplets are mobile and can fuse, which should be dependent on the measurement cycle and may be the reason for the increased measurement deviation (10.6%) in this case (see also Figure S4). For the measurements dominated by capillary forces, the statistical data shows a narrow, normal distribution with standard deviations in the range of 5−7% (Figure 3b).

These experiments demonstrate that the diamond colloidal probe technique is a valuable method for investigating the material surface or interface of differently terminated diamond. This plays a huge role in particular for bonding with other substrates.[33] It should be noted that for quantification of such forces, the environment, i.e., the humidity, should be well-controlled.[34] Our measurements were carried out on the same day at a relative humidity of approximately 40%.

Additionally, studies in solution were carried out that are less sensitive to surrounding conditions. In solution, meniscus forces can be excluded and hence characterization of electrostatic/double-layer, van der Waals (vdW) forces, and covalent binding are feasible. The colloids were attached to soft cantilevers and make measurements in the lower piconewton range possible. Thus, e.g., long-range electrostatic interactions can also be investigated.

Using an O-colloid, measurements on OPCD were carried out to investigate the influence of KCl salt concentration, as previous studies have shown influences on the assembly behavior of nanodiamonds.[21] From the DLVO theory, it is known that high salt concentrations screen electrostatic interactions.[35] By changing the concentration of the added salt, this can be used to influence the stability of colloidal suspensions, e.g., for diamond seeding solutions. The obtained results show a decreasing force range when increasing the KCl concentration in both approach and retract parts of the curve (Figure 4a). This decrease can be attributed to the decreasing electrostatic or double-layer forces.

The highest values of 183.9 ± 5.1 nm were obtained at a KCl concentration of 10^{-5} M (Note: This value is obtained by determining an increase in the repulsive force by more than 25 pN). When increasing the concentration, the range decreases to 77.1 ± 3 nm for 10^{-4} M, 20.1 ± 1.6 nm for 10^{-3} M, and 5.0 ± 1.3 nm for 10^{-2} M (Figure 4b). As observed before, the obtained values show narrow normal distributions, which indicate stable measurement conditions.

The inset in Figure 4a shows representative approach curves of the measurement. For low concentrations, the repulsive force goes up to approximately 600 pN before short-range attractive forces (vdW) dominate and a snap-in to the surface occurs. This force is strongly decreasing when reaching 10^{-3} M as attraction outweighs the long-range repulsion (electrostatics/double-layer forces). As these measurements are not only influenced by electrostatics, they can be described using the DLVO theory. Fits of the presented data reveal changes in surface potential and charge depending on the salt concentration (see Figure S6 and Table S2). The obtained

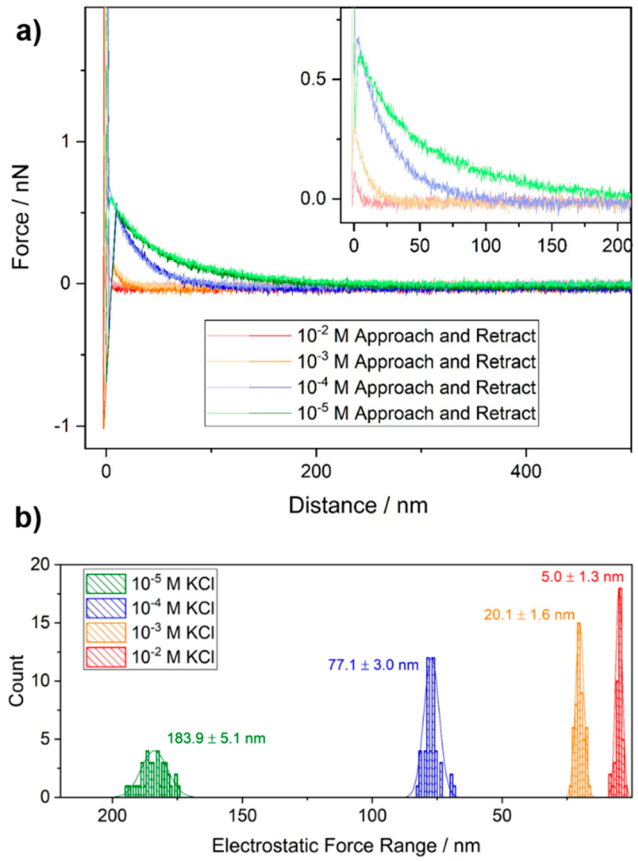

Figure 4. Force spectroscopic measurements using O-terminated colloids and diamond samples in solution. (a) Representative force curves at different KCl concentrations (inset shows magnified view of the approach traces). (b) Statistical data of the force range (repulsion >25 pN) with dependence on the KCl concentration.

information is important, e.g., to get insight into diamond-based ion sensitive field effect transistors (ISFETs).[36] However, it should be noted that at high salt or surfactant concentrations, where the Debye length is smaller than the roughness, standard DLVO theory may not be applicable without taking the roughness into account.[37] Concerning the adhesion, these measurements show the strong influence of meniscus forces in air in the previous measurements (Figure 3). Whereas the adhesion of the O-colloid on OPCD in air was as high as 20 nN, the adhesion in solution is only around 1 nN (Figure 4a). This is caused by the electrostatic repulsion originating from the C−O dipole on both surfaces. The low adhesion also indicates that no covalent bonds are formed, e.g., by condensation, in the short contact time of approximately 10 ms.

CONCLUSIONS

This study demonstrates the usage of diamond spherical particles for probing surface mechanical properties and interactions using AFM. The novel technique is referred to as diamond colloidal probe force spectroscopy. It was shown that mechanical parameters like the Young's modulus can be obtained on soft substrates, which is particularly interesting for measurements in biological matrixes. Here, contamination and fouling impede long-term measurements, and diamond may provide a robust and biocompatible probe surface.[38] Measurements in air provide insight into the wettability properties of

DOI: 10.1021/acs.analchem.9b00693
Anal. Chem. 2019, 91, 5537−5541

this material after different surface treatments. Apart from that, measurements in solution are feasible, where, e.g., electrostatic and van der Waals forces can be investigated. This makes detailed studies on the surface chemistry and physics of diamond films possible, which can provide a better understanding of the diamond-material interface, e.g., for nanodiamond seeding processes that are commonly used to obtain thin film diamond coatings on a variety of substrates. The statistical evaluations showed narrow normal distributions that prove the robustness of the approach. Besides the presented experiments, the technique may be used to study nanotribological properties of diamond with different surface modifications like fluorine in the future. In addition, through boron doping, robust, micrometer-sized spheres have already been fabricated and will be used in future studies as spherical electrodes to make use of the excellent electrochemical properties of boron doped diamond electrodes.

■ ASSOCIATED CONTENT

Supporting Information

The Supporting Information is available free of charge on the ACS Publications website at DOI: 10.1021/acs.analchem.9b00693.

AFM and FIB characterization of the diamond colloidal probe, Young's modulus determination by Hertz and DMT fitting, hydrophobic interaction between H-Colloid and HPCD, SEM characterization of the used probes, and DLVO fitting of the force curves obtained in solution (PDF)

■ AUTHOR INFORMATION

Corresponding Author

*E-mail: peter.knittel@iaf.fraunhofer.de. Phone: +49-761-5159-324. Fax: +49-761-5159-71324.

ORCID

Peter Knittel: 0000-0002-2769-3615

Taro Yoshikawa: 0000-0001-9624-4971

Author Contributions

The manuscript was written through contributions of all authors.

Notes

The authors declare no competing financial interest.

■ ACKNOWLEDGMENTS

This work was supported by European Union's Horizon 2020 Research and Innovation Programme under Grant No. 665085 (DIACAT).

■ REFERENCES

(1) Kappl, M.; Butt, H.-J. *Part. Part. Syst. Charact.* **2002**, *19* (3), 129−143.

(2) McNamee, C. E.; Pyo, N.; Tanaka, S.; Vakarelski, I. U.; Kanda, Y.; Higashitani, K. *Colloids Surf., B* **2006**, *48* (2), 176−182.

(3) Tsapikouni, T. S.; Allen, S.; Missirlis, Y. F. *Biointerphases* **2008**, *3* (1), 1−8.

(4) Richard Bowen, W.; Doneva, T. A. *J. Colloid Interface Sci.* **2000**, *229* (2), 544−549.

(5) Fuji, M.; Machida, K.; Takei, T.; Watanabe, T.; Chikazawa, M. *Langmuir* **1999**, *15* (13), 4584−4589.

(6) Fielden, M. L.; Hayes, R. A.; Ralston, J. *Langmuir* **1996**, *12* (15), 3721−3727.

(7) Knittel, P.; Zhang, H.; Kranz, C.; Wallace, G. G.; Higgins, M. J. *Nanoscale* **2016**, *8* (8), 4475−4481.

(8) McNamee, C. E.; Pyo, N.; Higashitani, K. *Biophys. J.* **2006**, *91* (5), 1960−1969.

(9) Dörig, P.; Ossola, D.; Truong, A. M.; Graf, M.; Stauffer, F.; Vörös, J.; Zambelli, T. *Biophys. J.* **2013**, *105* (2), 463−472.

(10) Niedermann, P.; Hänni, W.; Morel, D.; Perret, A.; Skinner, N.; Indermühle, P.-F.; de Rooij, N.-F.; Buffat, P.-A. *Appl. Phys. A: Mater. Sci. Process.* **1998**, *66* (7), S31−S34.

(11) Avdic, A.; Lugstein, A.; Wu, M.; Gollas, B.; Pobelov, I.; Wandlowski, T.; Leonhardt, K.; Denuault, G.; Bertagnolli, E. *Nanotechnology* **2011**, *22* (14), 145306.

(12) Drew, M. E.; Konicek, A. R.; Jaroenapibal, P.; Carpick, R. W.; Yamakoshi, Y. *J. Mater. Chem.* **2012**, *22* (25), 12682.

(13) Rezek, B.; Ukraintsev, E.; Michalíková, L.; Kromka, A.; Zemek, J.; Kalbacova, M. *Diamond Relat. Mater.* **2009**, *18* (5−8), 918−922.

(14) Williams, O. A.; Hees, J.; Dieker, C.; Jäger, W.; Kirste, L.; Nebel, C. E. *ACS Nano* **2010**, *4* (8), 4824−4830.

(15) Maier, F.; Ristein, J.; Ley, L. *Phys. Rev. B: Condens. Matter Mater. Phys.* **2001**, *64* (16), 165411.

(16) Maier, F.; Riedel, M.; Mantel, B.; Ristein, J.; Ley, L. *Phys. Rev. Lett.* **2000**, *85* (16), 3472−3475.

(17) Zhu, D.; Zhang, L.; Ruther, R. E.; Hamers, R. J. *Nat. Mater.* **2013**, *12* (9), 836−841.

(18) Geisler, M.; Hugel, T. *Adv. Mater.* **2010**, *22* (3), 398−402.

(19) Gao, F.; Wolfer, M. T.; Nebel, C. E. *Carbon* **2014**, *80* (1), 833−840.

(20) Yoshikawa, T.; Gao, F.; Zuerbig, V.; Giese, C.; Nebel, C. E.; Ambacher, O.; Lebedev, V. *Diamond Relat. Mater.* **2016**, *63*, 103−107.

(21) Yoshikawa, T.; Zuerbig, V.; Gao, F.; Hoffmann, R.; Nebel, C. E.; Ambacher, O.; Lebedev, V. *Langmuir* **2015**, *31* (19), 5319−5325.

(22) Füner, M.; Wild, C.; Koidl, P. *Appl. Phys. Lett.* **1998**, *72* (10), 1149−1151.

(23) Butt, H.-J.; Jaschke, M. *Nanotechnology* **1995**, *6* (1), 1−7.

(24) Ruffinatto, S.; Girard, H. A.; Becher, F.; Arnault, J. C.; Tromson, D.; Bergonzo, P. *Diamond Relat. Mater.* **2015**, *55*, 123−130.

(25) Petrák, V.; Vlčková Živcová, Z.; Krýsová, H.; Frank, O.; Zukal, A.; Klimša, L.; Kopeček, J.; Taylor, A.; Kavan, L.; Mortet, V. *Carbon* **2017**, *114*, 457−464.

(26) Hertz, H. *J. für die reine und Angew. Math.* **1882**, *1882* (92), 156−171.

(27) Derjaguin, B. V.; Muller, V. M.; Toporov, Y. P. *J. Colloid Interface Sci.* **1975**, *53* (2), 314−326.

(28) Hoffmann, R.; Kriele, A.; Obloh, H.; Hees, J.; Wolfer, M.; Smirnov, W.; Yang, N.; Nebel, C. E. *Appl. Phys. Lett.* **2010**, *97* (5), 052103.

(29) He, M.; Szuchmacher Blum, A.; Aston, D. E.; Buenviaje, C.; Overney, R. M.; Luginbühl, R. *J. Chem. Phys.* **2001**, *114* (3), 1355−1360.

(30) Butt, H.-J.; Graf, K.; Kappl, M. *Physics and Chemistry of Interfaces*; Wiley-VCH Verlag GmbH & Co. KGaA: Weinheim, Germany, 2003.

(31) Ostrovskaya, L.; Perevertailo, V.; Ralchenko, V.; Dementjev, A.; Loginova, O. *Diamond Relat. Mater.* **2002**, *11* (3−6), 845−850.

(32) Cao, P.; Xu, K.; Varghese, J. O.; Heath, J. R. *Nano Lett.* **2011**, *11* (12), 5581−5586.

(33) Yushin, G. N.; Aleksov, A.; Wolter, S. D.; Okuzumi, F.; Prater, J. T.; Sitar, Z. *Diamond Relat. Mater.* **2004**, *13* (10), 1816−1821.

(34) Thormann, E. *Curr. Opin. Colloid Interface Sci.* **2017**, *27*, 18−24.

(35) Derjaguin, B.; Landau, L. *Prog. Surf. Sci.* **1993**, *43* (1−4), 30−59.

(36) Denisenko, A.; Jamornmarn, G.; El-Hajj, H.; Kohn, E. *Diamond Relat. Mater.* **2007**, *16* (4−7), 905−910.

(37) Zou, Y.; Jayasuriya, S.; Manke, C. W.; Mao, G. *Langmuir* **2015**, *31* (38), 10341−10350.

(38) Tang, L.; Tsai, C.; Gerberich, W. W.; Kruckeberg, L.; Kania, D. R. *Biomaterials* **1995**, *16* (6), 483−488.

DOI: 10.1021/acs.analchem.9b00693
Anal. Chem. 2019, 91, 5537−5541